

Aharonov-Bohm spectral features and coherence lengths in carbon nanotubes

S. Roche,^{1,2,*} G. Dresselhaus,³ M. S. Dresselhaus,^{4,†} and R. Saito⁵

¹*Departamento de Física Teórica, Universidad de Valladolid, E-47011 Valladolid, Spain*

²*Commissariat à l'Énergie Atomique, DRFMC/SPSMS, 38042 Grenoble, France*

³*Francis Bitter Magnet Laboratory, Massachusetts Institute of Technology, Cambridge, Massachusetts 02139*

⁴*Department of Physics and Department of Electrical Engineering and Computer Science, Massachusetts Institute of Technology, Cambridge, Massachusetts 02139*

⁵*Department of Electronic Engineering, University of Electro-communications, 1-5-1 Chofugaoka Chofu, Tokyo 182-8585, Japan*
(Received 24 April 2000; revised manuscript received 27 June 2000)

The electronic properties of carbon nanotubes are investigated in the presence of disorder and a magnetic field parallel or perpendicular to the nanotube axis. In the parallel field geometry, the ϕ_0 -periodic ($\phi_0 = hc/e$) metal-insulator transition induced in metallic or semiconducting nanotubes is shown to be related to a chirality-dependent shifting of the energy of the van Hove singularities (VHS's). The effect of disorder on this magnetic-field-related mechanism is considered with a discussion of mean free paths, localization lengths, and magnetic dephasing rate in the context of recent experiments.

The discovery of multiwall carbon nanotubes (CN's) by Iijima¹ has triggered a huge amount of activity from basic research to applied technologies.² Indeed, CN's have unique physical properties, from their light weight and record-high elastic modulus, to their geometry-dependent electronic states. Lately, there has been increasing industrial interest in CN properties for their applicability to flat displays, fiber reinforcement technologies, carbon-based nanotips,³ and future CN-based molecular electronic devices.⁴ CN's consist of coaxially rolled graphene sheets determined by only two integers (n, m) , and depending on the choice of chirality, metallic or semiconducting behavior is exhibited for systems with typical radii of 0.5 to 20 nm and lengths of several micrometers. The study of the influence of a magnetic field and topological defects⁵ or chemical (e.g., substitutional⁶) disorder is a current subject of concern, since disorder can strongly affect the generic properties of CN-based devices, such as field effect transistors.⁷⁻⁹

Conductivity measurements have been performed on bundles of single-walled carbon nanotubes using scanning tunneling microscopy (STM).¹⁰ By moving the tip along the length of the nanotubes, sharp deviations in the I - V characteristics could be observed and related to theoretically predicted electronic properties.^{2,11,12} In particular, the partition of the spectrum into a complex van Hove singularity (VHS) pattern is a remarkable feature. At energies where VHS's occur, the band velocities tend to zero, which is a manifestation of confined states, generally seen in one- (1D) or two-dimensional (2D) systems. It is thus expected that the presence of VHS's (their distribution and number) also affect the physical properties of CN's. Recently it has been shown that from the VHS patterns, one could distinguish between different nanotube chiralities,¹³ which is an interesting approach for obtaining a more precise knowledge of the effect of geometry on the physical properties of CN's, such as transport.

In this context, experiments with a magnetic field perpendicular¹⁴⁻¹⁶ or parallel to the nanotube axis¹⁷ have been performed, and in the latter case, $\phi_0/2$ -periodic (where ϕ_0 is a flux quantum) Aharonov-Bohm oscillations of the

magnetoconductance have been found,¹⁷ suggesting rather short electronic coherence lengths. Fujiwara *et al.*¹⁸ also observed a surprising $\phi_0/3$ oscillation in the magnetoconductance and related this periodic behavior to a superposition of phase shifts due to spectral effects, assuming three internal tubes with different chiralities. In the following, we propose to clarify the effect of a magnetic field on the density of states (DOS) with respect to the field orientation relative to the nanotube axis, and the influence that disorder, as featured by random site energies, may have on these magnetic field effects. We further derive some criteria for estimating the mean free path and localization length qualitatively in this general context.

I. SPECTRAL PROPERTIES OF METALLIC AND SEMICONDUCTING CN'S

Without a magnetic field and disorder, the electronic properties of nanotubes are known to be dependent on their chiral vector $\vec{C}_h = (n, m)$, expressed in unit vectors of the hexagonal lattice by $|\vec{C}_h| = \sqrt{3}a_{C-C}\sqrt{n^2 + m^2 + nm}$ ($a_{C-C} = 1.42$ Å). From a tight-binding description of the graphite π bands, with only first-neighbor C-C interactions, the dispersion relations can be obtained by diagonalization of the Hamiltonian (with periodic boundary conditions), and, for instance, for the case of armchair (n, n) nanotubes, we can write²

$$\varepsilon_{\pm}(k_{\perp}, k_{\parallel}) = \pm \gamma_0 \left\{ 1 \pm 4 \cos \frac{k_{\perp} a}{2} \cos \frac{\sqrt{3} k_{\parallel} a}{2} + 4 \cos^2 \frac{k_{\perp} a}{2} \right\}^{1/2}, \quad (1)$$

where γ_0 is the energy overlap integral between carbon atoms, $a = \sqrt{3}a_{C-C}$ is the graphite lattice constant, and k_{\perp} is the wave vector perpendicular to the nanotube axis $k_{\perp} = 2\pi q/(\sqrt{3}na)$, where $q = 1, \dots, 2n$, giving the quantized

values of the wave vector in the \vec{C}_h direction, whereas the wave vector k_{\parallel} parallel to the nanotube axis is associated with the specification of the wave vectors in 1D Brillouin zone $-\pi/\sqrt{3} < k_{\parallel}a < \pi/\sqrt{3}$, which defines the 1D-band dispersion. By expanding the dispersion relations around the \vec{K} points (i.e., close to the Fermi energy), with small $\delta\vec{k} = \vec{k} - \vec{K} = (2\pi/|\vec{C}_h|)(q - \nu/3)\vec{k}_{\perp} + \delta k_{\parallel}\vec{k}_{\parallel}$ (with $\vec{T} \cdot \vec{k}_{\parallel} = 2\pi$ and $\vec{T} \cdot \vec{k}_{\perp} = 0$, where \vec{T} is the smallest translation vector along the tube axis), one finds²

$$\varepsilon_{\pm}(\delta k) = \pm \frac{\sqrt{3}\gamma_0}{2} \sqrt{\left\{ \frac{2\pi a}{|\vec{C}_h|} \left(q - \frac{\nu}{3} \right) \right\}^2 + |\delta k_{\parallel}|^2}, \quad (2)$$

where the integer ν is related to m and n by $n - m = 3p + \nu$, with $p = 0, 1, 2, \dots$ and $\nu = 0, \pm 1$. Two bands may then cross at the Fermi level according to the value of ν . If $\nu = \pm 1$ (i.e., $n - m = 3p \pm 1$), one gets $\Delta_g = \varepsilon_{+}(\delta k) - \varepsilon_{-}(\delta k) = 2\pi a_{C-C}\gamma_0/|\vec{C}_h|$, which defines the gap at the Fermi energy of a semiconducting nanotube. For $\nu = 0$ (i.e., $m - n = 3p$), the system is metallic (in the sense $\Delta_g = 0$). Typically, the gap energy Δ_g is, respectively, in the range $1.65 < \Delta_g < 0.27$ eV for nanotube diameters d_{nt} in the range $0.5 < d_{nt} < 3$ nm. Predicted theoretically,^{2,19} these results have been confirmed experimentally by scanning tunneling spectroscopy (STM) measurements.^{8,20-22}

II. MAGNETIC-FIELD-INDUCED METAL-INSULATOR TRANSISTOR, SPLITTING, AND SHIFTING OF VHS'S

A. Magnetic field parallel to the tube axis

To investigate Aharonov-Bohm phenomena, we start from the Hamiltonian $\mathcal{H}_{\mathbf{k}\mathbf{k}'}$ for electrons moving on a nanotube under the influence of a magnetic field:^{2,23,24}

$$\mathcal{H}_{\mathbf{k}\mathbf{k}'} = \frac{1}{N} \sum_{\mathbf{R}, \mathbf{R}'} e^{-i(\mathbf{k} \cdot \mathbf{R} - \mathbf{k}' \cdot \mathbf{R}') - (ie/\hbar)\Delta\varphi_{\mathbf{R}, \mathbf{R}'}} \times \left\langle \psi(\mathbf{r} - \mathbf{R}) \left| \frac{\mathbf{p}^2}{2m} + V \right| \psi(\mathbf{r} - \mathbf{R}') \right\rangle, \quad (3)$$

where the phase factors are given by

$$\Delta\varphi_{\mathbf{R}, \mathbf{R}'} = \int_0^1 (\mathbf{R}' - \mathbf{R}) \cdot [\mathcal{A}(\mathbf{R} + \lambda[\mathbf{R}' - \mathbf{R}])] d\lambda, \quad (4)$$

$|\psi(\mathbf{r} - \mathbf{R}')\rangle$ is the localized atomic orbital, and \mathbf{p} and V are, respectively, the momentum and disorder potential operators. As shown hereafter, different physics is found according to the orientation of the magnetic field with respect to the nanotube axis. In the former case, the vector potential is simply expressed as $\mathcal{A} = (\phi/|\vec{C}_h|, 0)$ in the two-dimensional $(\vec{C}_h/|\vec{C}_h|, \vec{T}/|\vec{T}|)$ coordinate system, and the phase factors become $\Delta\varphi_{\mathbf{R}, \mathbf{R}'} = i(\mathcal{X} - \mathcal{X}')\phi/|\vec{C}_h|$ for $\mathbf{R} = (\mathcal{X}, \mathcal{Y})$. This yields new magnetic-field-dependent dispersion relations $\varepsilon(\delta k, \phi/\phi_0)$. Close to the Fermi energy, this energy disper-

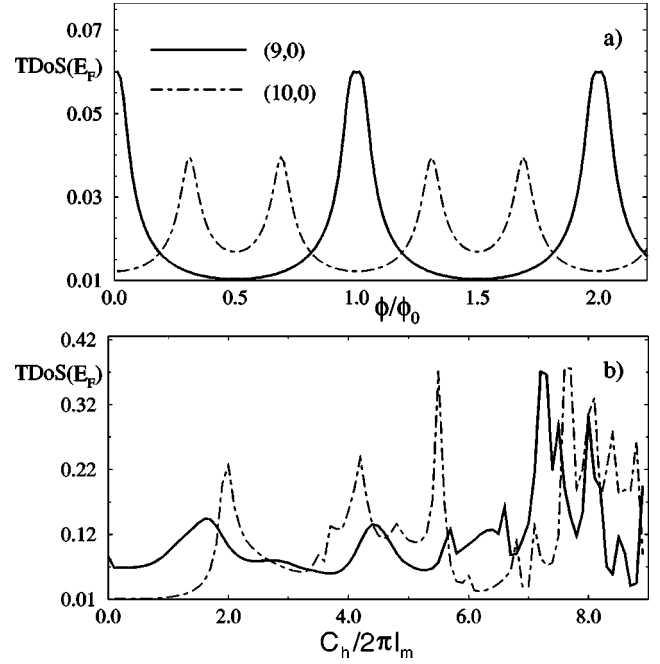


FIG. 1. (a): TDOS(states/eV per 1C atom) at the Fermi level as a function of the magnetic field parallel to the nanotube axis in units of ϕ/ϕ_0 for (9,0) (solid line) and (10,0) (dash-dotted line) nanotubes. (b): TDOS(states/eV per 1C atom) at the Fermi level as a function of $|\vec{C}_h|/2\pi l_m$ for a magnetic field perpendicular to the nanotube axis, where $l_m = \sqrt{\hbar c/eB}$ is the magnetic length and for (9,0) (solid) and (10,0) (dash-dot) nanotubes.

sion relation is affected according to $k_{\perp} \rightarrow k_{\perp} + 2\pi\phi/(\phi_0|\vec{C}_h|)$, which leads to a ϕ_0 -periodic variation²³⁻²⁵ of the energy gap Δ_g . Such patterns are reported in Fig. 1 (top) where the total density of states (TDOS) at the Fermi level is plotted as a function of magnetic field strength ϕ/ϕ_0 threading the nanotube for the metallic (9,0) and the semiconducting (10,0) nanotubes. Note that a finite DOS is found in Fig. 1 for semiconducting and metallic nanotubes as a function of magnetic field, since we consider that the Green's function has a finite imaginary part, that we use to calculate the DOS by a recursion method.²⁶

In the semiconducting case, the oscillations in the DOS correspond to the following variations of the gap widths:²⁵

$$\Delta_g = \begin{cases} \Delta_0 \left| 1 - 3 \frac{\phi}{\phi_0} \right| & \text{if } 0 \leq \phi \leq \frac{\phi_0}{2} \\ \Delta_0 \left| 2 - 3 \frac{\phi}{\phi_0} \right| & \text{if } \frac{\phi_0}{2} \leq \phi \leq \phi_0, \end{cases} \quad (5)$$

where $\Delta_0 = 2\pi a_{C-C}\gamma_0/|\vec{C}_h|$ is a characteristic energy associated with the nanotube. It turns out that at ϕ values of $\phi_0/3$ and $2/3\phi_0$, in accordance with the values of $\nu = \pm 1$, there is a local gap closing in the vicinity of either the K or K' points in the Brillouin zone. This can be seen simply by considering the coefficients of the general wave function in the vicinity of the K and K' points, which can be written as $\Psi_{\vec{K} + \delta\vec{k}_K}(\vec{r} + \vec{C}_h)$. Since periodic boundary conditions apply in the \vec{C}_h direction, one can write $\exp[i(\vec{K} + \delta\vec{k}_K) \cdot \vec{C}_h] = 1$. For $\nu = +1$, we write $\delta\vec{k}_K = (2\pi/|\vec{C}_h|)(q - 1/3)\vec{k}_{\perp} + \delta k_{\parallel}\vec{k}_{\parallel}$, whereas

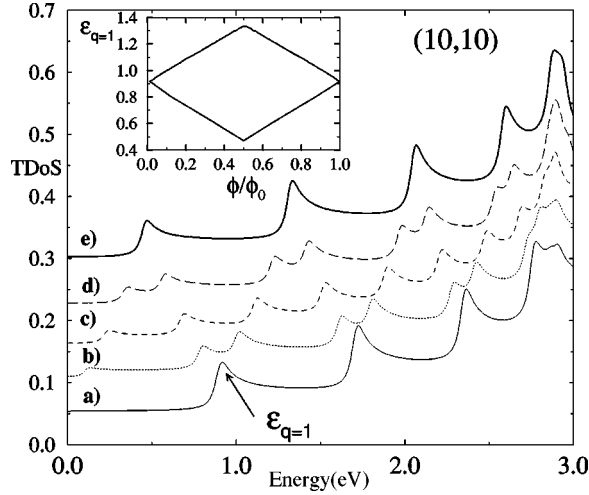


FIG. 2. TDOS (states/eV per 1C atom) of a metallic armchair (10,10) nanotube as a function of Fermi energy for $\phi/\phi_0 = (a)$ 0.0, (b) 0.125, (c) 0.25, (d) 0.375, and (e) 1/2. Note that curves b , c , d , and e have been upshifted for the sake of clarity. The inset shows the evolution of the first VHS position (energy in units of eV) over the complete oscillation cycle, initially located at 0.896 eV for $\phi/\phi_0 = 0$.

$\delta\vec{k}_{K'} = (2\pi/|C_h|)(q+1/3)\vec{k}_\perp + \delta k_\parallel\vec{k}_\parallel$. When $K \rightarrow K'$, then $\pm 1/3 \rightarrow \mp 1/3$ in the above expressions, as ν goes from $+1 \rightarrow -1$, which makes the situation between K and K' symmetrical. Similarly for metallic nanotubes, the gap width Δ_g is expressed by²⁵

$$\Delta_g = \begin{cases} 3\Delta_0 \frac{\phi}{\phi_0} & \text{if } 0 \leq \phi \leq \frac{\phi_0}{2} \\ 3\Delta_0 \left|1 - \frac{\phi}{\phi_0}\right| & \text{if } \frac{\phi_0}{2} \leq \phi \leq \phi_0. \end{cases} \quad (6)$$

Here we show that the magnetic field also affects the positions of the VHS's over the entire spectrum, which may be experimentally observed. As an illustration, the TDOS for a (10,10) tube without a magnetic field, shown as curve (a) in Fig. 2, is compared to the magnetic field case with $\phi/\phi_0 = 0.125, 0.25, 0.375,$ and 0.5 [shown in Fig. 2 as curves $(b), (c), (d),$ and (e) , respectively] for energies up to 3 eV in which we have taken $\gamma_0 = 2.9$ eV, which is suitable for comparison with experiments.^{13,27} To understand such effects, one calculates the TDOS from

$$\text{Tr}[\delta(E - \mathcal{H})] = \frac{2}{2\pi} \sum_n \int dk \delta(E - \varepsilon_{nk}), \quad (7)$$

where the sum is taken over the n energy bands ε_{nk} and we use

$$\left| \frac{\partial \varepsilon(\delta k, \phi/\phi_0)}{\partial k_\perp} \right|^{-1} = \frac{2}{\sqrt{3}\gamma_0 a} \frac{|\varepsilon(\delta k, \phi/\phi_0)|}{\sqrt{\varepsilon^2(\delta k, \phi/\phi_0) - \varepsilon_q^2}}, \quad (8)$$

where ε_q indicates the position (energy) of the VHS's. We can rewrite the DOS as

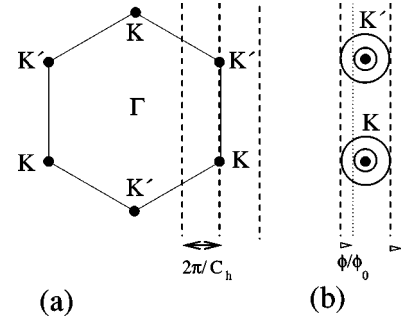


FIG. 3. (a) Brillouin zone of 2D graphite and typical lines (dashed lines) defining the energy bands near the K points for an armchair nanotube. (b) Some equienergy contours around the K and K' points (circles) as well as an illustration of the VHS shifting process. While one VHS gets closer to lower energy (closer to the Fermi energy at the K and K' points), the other VHS initially symmetrical, flows to higher energy.

$$\rho(E) = \frac{2a}{\pi\gamma_0|\vec{C}_h|} \sum_{q=1}^{2n} \delta_q(E, \varepsilon_q), \quad (9)$$

where $\delta_q(E, \varepsilon_q) = |E|/\sqrt{E^2 - \varepsilon_q^2}$ for $|E| > |\varepsilon_q|$ and zero otherwise.²⁸

The ε_q denote the energy-positions of the VHS's, and for armchair nanotubes (n, n) , one finds that $\varepsilon_q = \pm \gamma_0 \sqrt{1 + 3 \cos^2 q\pi/n}$ and $\varepsilon_q = \pm \gamma_0 \sqrt{1 - \cos^2 q\pi/n}$ define the whole set of VHS's ($q = 1, \dots, 5$). The magnetic field induces a shift of k_q by a factor $2\pi\phi/(\phi_0|\vec{C}_h|)$, which results in a new expression for the quantized values of the wave vector in the \vec{C}_h direction, which reads $2\pi(q + \phi/\phi_0)/|\vec{C}_h|$. For the metallic (10,10) nanotube, an energy gap thus opens at the Fermi level, whose width Δ_g is proportional to the magnetic strength for $\phi/\phi_0 \leq 1/2$. Given that ε_q is a function of k_q , a shift of the energy positions of the VHS's follows, as well as the breaking of the degeneracy of a pair of K and K' points contributing to a given VHS, as explained below. In the (10,10) nanotube, the first five VHS's (which each have a degeneracy of 4) are simply given by $\varepsilon_q = \gamma_0 \sin(\pi q/10)$ ($q = 1, \dots, 5$), which leads to $\varepsilon_{q=1} = 0.896$ eV, $\varepsilon_{q=2} = 1.705$ eV, $\varepsilon_{q=3} = 2.346$ eV, $\varepsilon_{q=4} = 2.758$ eV, and $\varepsilon_{q=5} = 2.900$ eV. Thereby, phase shifts induced by the magnetic field correspond simply to

$$\varepsilon_q = \gamma_0 \sin\left\{ \frac{\pi}{10} \left(q \pm \frac{\phi}{\phi_0} \right) \right\}. \quad (10)$$

This is illustrated in Fig. 2, which gives the evolution of the TDOS of a (10,10) nanotube close to some VHS.

At low field, the degeneracy of the K and K' points is broken as illustrated in Fig. 3, which shows the Brillouin zone for 2D graphite along with the equienergy contours around K and K' points, so that in addition to the upshift of one component of the degenerate zero-field VHS's, the other magnetically split component is correspondingly downshifted. Both VHS's move apart up to $\phi/\phi_0 = 1/2$, where the two originally different VHS's merge into one. The positions of such merged VHS's are related to a $\cos k_q a/2$ factor (that is, through a $\cos 2\pi\phi/\phi_0$ factor), so that a further increase of the magnetic field strength yields an opposite shifting of the

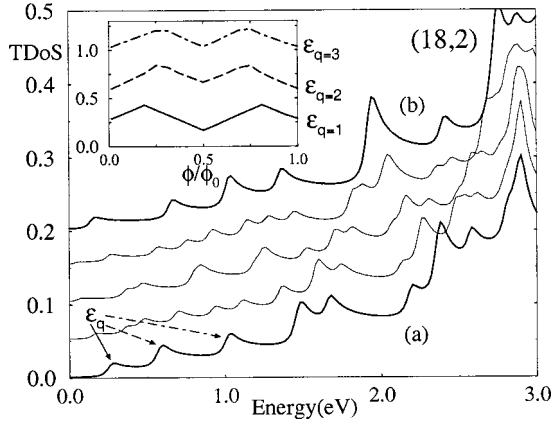


FIG. 4. TDOS of an (18,2) tube as a function of the Fermi energy for several values of the magnetic flux, from (a) zero flux to (b) $\phi_0/2$ flux, and intermediate cases corresponding to Fig. 2. The inset shows the evolution of the position of three VHS's (as pointed out by arrows) versus normalized magnetic flux.

VHS positions, and at $\phi/\phi_0=1$, the initial positions of the VHS's are recovered, along with their degeneracy (those given at $\phi/\phi_0=0$), and a gap closing thus results. At low magnetic field since $\varepsilon_q \sim \phi/\phi_0$, the shift of the VHS's position for a given magnetic field is proportional to ϕ/ϕ_0 for all VHS's. In the inset of Fig. 2, the positions of the VHS's originally at 0.896 eV (for zero field) are given as a function of the normalized magnetic flux. The splitting is illustrated and a strong shift of the lowest VHS, by ~ 0.4 eV, is predicted at half a quantum flux. Note that the upshifted and downshifted components are symmetrical with respect to the ϕ/ϕ_0 axis.

The TDOS of the semiconducting (18,2) nanotube is also investigated and displays similar features, as exemplified by Fig. 4. The inset gives the shifting of the energy position of the three VHS's closest to the Fermi level as a function of normalized magnetic flux. An interesting $\phi_0/2$ symmetry is clearly seen for semiconducting tubes, as in the former case (Fig. 2) for metallic nanotubes. These interesting effects of the magnetic field on the spectral structure has, to our knowledge, not been explicitly investigated experimentally up to now, but recent progress in the observation of room temperature resonant Raman spectra for purified single-wall nanotubes can disclose fine structure in the DOS, through the enhancement of the intensity of optical absorption at the energies associated with VHS's.²⁹ Magneto-optical techniques could then provide a possible way to test the above predictions. To that end, we give here the predicted energy position shifts for the VHS's closest to the Fermi energy, which are related to the phase shift induced by magnetic flux variations from 0 to $\phi_0/2$ for nanotubes with diameters $d_1=1.8$ nm [the largest single-walled nanotube (SWNT) made up to now], $d_2=6$ nm and $d_3=8$ nm [corresponding to typical multiwalled nanotube (MWNT) outer diameters] and corresponding to (n,n) armchair tubes. The predicted energy position shift is given by

$$\Delta\varepsilon_{q=1}\left(0, \frac{1}{2}\right) = \varepsilon_{q=1}\left(\frac{\phi_0}{2}\right) - \varepsilon_{q=1}(0) = \gamma_0 \left(\sin \frac{3\pi}{2n} - \sin \frac{\pi}{n} \right), \quad (11)$$

which implies $\Delta\varepsilon_{q=1}^1 = 173$ meV, $\Delta\varepsilon_{q=1}^2 = 52.3$ meV, and $\Delta\varepsilon_{q=1}^3 = 39.2$ meV, and the corresponding magnetic field strengths at $\phi_0/2$ are $B_1 \sim 200$ T, $B_2 \sim 18$ T, and $B_3 \sim 10$ T, which are within the scope of present experimental capabilities [we take $B = (2\pi\phi_0)/(3na)^2$, and $\phi_0 = 4.1356 \times 10^{-15}$ Tm²]. Note that the effect of the magnetic field should be observed for individual MWNT's, since the intertube coupling for MWNT's is believed to affect the electronic spectrum only weakly.

Whereas the splitting is universal for all tubes (chiral and achiral), in the most general case, the van Hove singularity shift will depend on the chirality, and on the applied magnetic field strength (not the position of the van Hove singularity). To estimate the corresponding shift, one may proceed in the following manner: given a chiral vector $\vec{C}_h = (n, m)$, one calculates the associated vectors \vec{k}_{\parallel} and \vec{k}_{\perp} which are drawn in the Brillouin zone.

This is here illustrated for the (10,10) armchair nanotube for which $\vec{k}_{\perp} = (-t_2\vec{b}_1 + t_1\vec{b}_2)/N_{(10,10)} = (\vec{b}_1 + \vec{b}_2)/N_{(10,10)}$ with $N_{(10,10)} = 20$, the number of hexagons within the unit cell of a (10,10) nanotube, and \vec{b}_i the basis vector in reciprocal space (see Ref. 2), where the direction \vec{k}_{\perp} is found to be perpendicular to the $K-K'$ axis (Fig. 3), and the spacing between lines is equidistant to a given K point. For the (18,2) chiral nanotube with $N_{(18,2)} = 364$, we find $\vec{k}_{\perp} = (19\vec{b}_1 + 11\vec{b}_2)/N_{(18,2)}$, which defines another direction and spacing. No lines cross at the K and K' points, and the spacings between two consecutive lines are not equidistant to the K location (in fact the K point always appears to be one-third of the distance between the two lines near the Fermi energy). This affects the splitting, for instance, at the field corresponding to half a quantum flux unit, the pattern for the (18,2) nanotube is less simpler than that for the (10,10) nanotube but it can be evaluated systematically.

B. Magnetic field perpendicular to the tube axis

For a magnetic field perpendicular to the nanotube axis, the situation is more cumbersome, due to a site-position dependence of the vector potential. No apparent symmetries for the Aharonov-Bohm interferences on the nanotube are found in this case, and indeed, even if semiconducting nanotubes can become metallic with increasing magnetic field strength, nonperiodic oscillations are found, as described below. For \vec{B} normal to the tube axis, one starts from a vector potential, given in the two-dimensional coordinate system (\vec{C}_h, \vec{T}) , by

$$\mathcal{A} = \left(0, \frac{B|\vec{C}_h|}{2\pi} \sin \frac{2\pi}{|\vec{C}_h|} \mathcal{X} \right). \quad (12)$$

The effect of the magnetic field is driven by the phase factors introduced into the hopping integrals between two sites \mathbf{R}_i and \mathbf{R}_j [with $\mathbf{R}_i = (\mathcal{X}_i, \mathcal{Y}_i)$], and the phase factor $\Delta\varphi_{\mathbf{R},\mathbf{R}'}$ can be deduced from the Peierls substitution as follows:

$$\Delta\varphi_{\mathbf{R},\mathbf{R}'} = \begin{cases} \left(\frac{|\vec{C}_h|}{2\pi} \right)^2 B \frac{\Delta\mathcal{X}}{\Delta\mathcal{Y}} \left[\cos \frac{2\pi}{|\vec{C}_h|} \mathcal{X} - \cos \frac{2\pi}{|\vec{C}_h|} (\mathcal{X} + \Delta\mathcal{X}) \right] & (\Delta\mathcal{X} \neq 0) \\ \frac{|\vec{C}_h|}{2\pi} B \Delta\mathcal{Y} \sin \frac{2\pi}{|\vec{C}_h|} \mathcal{X} & (\Delta\mathcal{X} = 0) \end{cases} \quad (13)$$

where $\Delta\mathcal{X} = \mathcal{X}_i - \mathcal{X}_j$ and $\Delta\mathcal{Y} = \mathcal{Y}_i - \mathcal{Y}_j$.² In Fig. 1(b), we show the TDOS at the Fermi level ($E_F = 0$) as a function of the effective magnetic field defined by $\nu = |\vec{C}_h|/2\pi l_m$, where $l_m = \sqrt{\hbar c/eB}$ is the magnetic length. At low fields, the TDOS of metallic (9,0) and semiconducting (10,0) nanotubes at the Fermi level increases with the magnetic field strength. For higher values of magnetic field, our results are in agreement with previous results obtained by exact diagonalization.² Also Landau bands are generated for values for which $\nu \geq 2$. The aperiodic fluctuations of the TDOS are stronger at higher fields, with occasional low values of the DOS, reminiscent of a nonzero TDOS for the semiconducting nanotubes at the zero-field value.

In Fig. 5, several values of ν are considered for an initially semiconducting nanotube. For $\nu = 1$ the radius of the nanotube equals the magnetic length. Landau levels emerge whenever the magnetic length becomes smaller than the nanotube circumference length.¹⁹ Comparison of the case of $\nu = 3.5$ in Fig. 5 with the zero-field limit is instructive, since the VHS partition of the spectra has been totally replaced by a Landau-level spectrum (here, one can recognize square-root singularities for the VHS's, and a Lorentzian-shape singularity for the Landau levels). This transition from the VHS pattern to the Landau-level pattern is, however, more unlikely to be observed experimentally, since its observation requires a very high magnetic field.

III. DISORDER AND MAGNETIC FIELD EFFECTS

The effect of Anderson-type disorder on the electronic properties in addition to the presence of a magnetic field (parallel to the tube axis) is now addressed in order to investigate how disorder alters the VHS pattern and the metal-insulator transition (MIT), and how disorder qualitatively modifies the localization properties of the nanotubes when the system remains metallic. We consider here only the case of the metallic zigzag nanotube (9,0), but similar results are obtained for other metallic or semiconducting nanotubes. In zero magnetic field, this problem of localization in nanotubes has recently attracted a great deal of attention.³⁰⁻³³

The effect of randomness is considered by taking the site energies of the tight-binding Hamiltonian at random in the interval $[-W/2, W/2]$ (γ_0 unit), with a uniform probability distribution. Accordingly, the strength of the disorder is measured by W .

In Fig. 6 (for $\phi/\phi_0 = 1/2$), the TDOS for $W = 0.25$ up to $W = 2$ (1/3 of the total bandwidth) shows that disorder does not modify the gap at the Fermi level, even when the confinement effects disappear (vanishing of VHS's). Disorder obviously leads to a mixing of energy levels, which results in a vanishing of the VHS at $W = 1$ in our simulations. The gap

is more resistant to disorder, even when its strength is as large as 1/3 the total bandwidth. Thus magnetic effects are not affected by low levels of disorder, which is an interesting result, since it is believed that many defects or sources of weak scattering should be present in real nanotubes.

The estimation of the electron mean free path l_e in nanotubes is relevant for determining which is the most likely transport regime (ballistic versus diffusive), and further tells us whether or not the conductance should be quantized. While some experiments have observed conductance quantization,³⁴ others suggest, in contrast, rather short electronic coherence lengths.^{16,17} A calculation of l_e for armchair nanotubes has been performed using the special symmetries of these systems.³⁵ Here, we show that a simple recourse to the relaxation time approximation (RTA) in the limit of weak scattering is sufficient to give a fair estimate of l_e for both metallic chiral or achiral tubes, in qualitative agreement with prior results,³⁵ demonstrated for the armchair case.

Within the RTA, one can write $l_e = v_F \tau_e = \hbar v_F / [2 \text{Im} \Sigma(E_F)]$, where v_F is an average of the group velocity over the Fermi surface, τ_e is the mean free time, and $\Sigma(E_F)$ is the self-energy due to scattering events. The calculation of the electronic velocity is performed by a linearization of the dispersion relations in the vicinity of the Fermi level. For all metallic nanotubes, one finds to the lowest order of approximation that $\sqrt{\langle v_k^2 \rangle} = v_F = \sqrt{3} a \gamma_0 / 2\hbar$, which leads typically to $v_F = 8.5 \times 10^5 \text{ m s}^{-1}$. On the other hand, in the vicinity of the Fermi level, the density of states is given by

$$\begin{aligned} \rho(E) &= \text{Tr}[\delta(E - \mathcal{H})] \\ &= \frac{2}{\tilde{V}} \sum_n \int dk \delta(k - k_n) \left| \frac{\partial \varepsilon_{nk}}{\partial k} \right|^{-1} \\ &= \frac{2}{\pi \gamma_0 \sqrt{n^2 + m^2 + nm}}, \end{aligned} \quad (14)$$

where $\tilde{V} = \Delta k |\vec{C}_h| / 2\pi$ is the volume of k space per allowed k value, divided by the spacing between lines for these allowed values.

The application of the Fermi golden rule yields $\text{Im} \Sigma(E_F) \sim \langle \varepsilon_i^2 \rangle \langle G_0(i, i, E_F) \rangle \sim \pi W^2 \rho(E_F)$, where W is the disorder bandwidth and $\langle G_0(i, i, E_F) \rangle$ is the average of the local on-site ($|i\rangle$) Green's function elements. An estimate of the carrier mean free path (identical for metallic nanotubes with the same radius) is

$$l_e \approx \frac{3\sqrt{3} a \gamma_0^2}{2W^2} \sqrt{n^2 + m^2 + nm}. \quad (15)$$

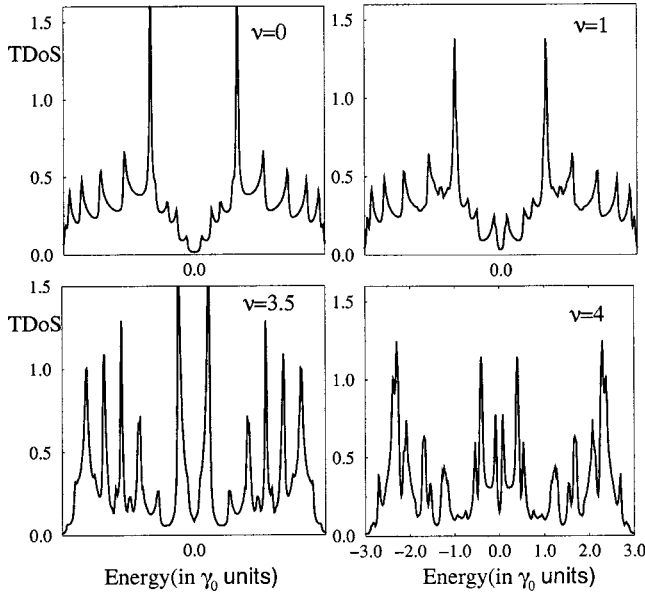


FIG. 5. TDOS of a (10,0) nanotube as a function of the Fermi energy for different values of magnetic field, perpendicular to the nanotube axis and with strength $\nu = |\vec{C}_h|/(2\pi l_m)$.

The important result that l_e is proportional to the nanotube diameter is relevant to the fact that the DOS at the Fermi energy decreases with increasing diameter. Accordingly, for a given disorder acting as a weak perturbation coupling some eigenstates to others close to Fermi surface, there are less available states to be scattered into, as the tube diameter decreases, yielding an enhancement of the mean free path. For instance, for (9,0) and (10,10) CN's, with respective diameters 0.7 nm and 1.37 nm, the corresponding mean free paths are estimated to be 0.9 μm and 1.8 μm , which are much larger than the circumference length and are about the typical length of the systems themselves (for a reasonable disorder $W \sim 0.2$ eV suggested by Ref. 35).

In experiments on SWNT's, or MWNT's in the metallic-like regime (i.e., with an Ohmic temperature dependence of the resistivity), the resistivity should scale as $\rho(d_{nt}) \sim 1/d_{nt}$ for a given temperature, where d_{nt} is the tube diameter. It would be interesting to analyze the departure from this law as the diameter of the MWNT's increases, since such departures would indicate a participation of the inner tubes to the measured transport regime. In particular, some activation transport process of inner semiconducting tubes may contribute or not, depending on the temperature and thus producing superimposed $\rho(d_{nt}) \sim \exp(\alpha_0 d_{nt})$ factors (where α_0 is a constant).

One notes that the Fermi golden rule does not include the quantum interferences that lead to localization. As nanotubes are basically 1D systems, from their estimated mean free paths, one can estimate the localization lengths at the Fermi level following the Thouless argument.³⁶ In thin wires, Thouless argued that by writing $R \sim 2\hbar/e^2$ for the resistance, there should be a transition to a localized state and an exponential increase of the resistance R . Consequently, from the resistance $R = 1/G = (1/\sigma)L^{2-D}$ (G is the conductance, σ the conductivity, and D the dimension of the system), assuming that the conductivity is calculated for a free electron gas in the wire [$\sigma = (e^2/\hbar)k_F l_e/3\pi^2$], it is straightforward to de-

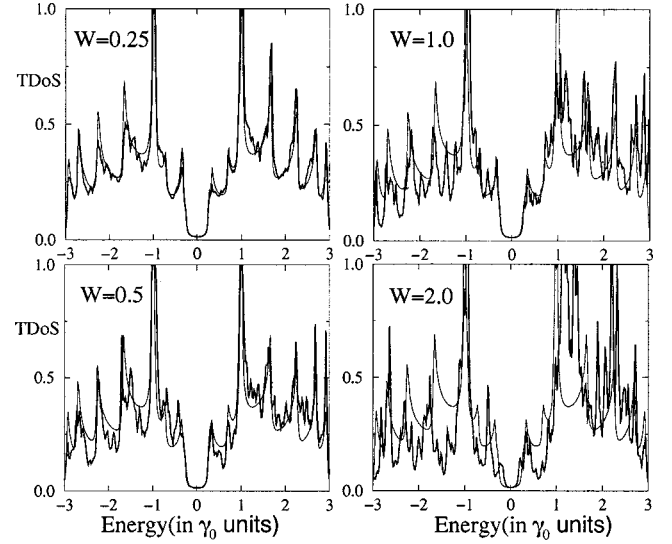


FIG. 6. TDOS as a function of the energy for $\phi/\phi_0 = 1/2$ and different values of the disorder strength W (in γ_0 unit). Thin lines give the zero-disorder case for comparison.

duce the localization length $\xi = (2Ak_F^2 l_e)/3\pi^2$ (we take $A = L^{D-1}$ as the cross section of the wire and $L = \xi$ at the wire length for which $R = 2\hbar/e^2$). Rewriting the last expression as $\xi = (A/\lambda_F^2)l_e$, the localization length ξ is shown to be related to the approximate number of independent electrons (with spatial extension $\sim \lambda_F^2$, where λ_F is the Fermi wavelength) which can be accommodated through the cross section of the wire times the average mean free path.

Nanotubes are hollow cylinders that lead to confinement effects in the direction perpendicular to the tube axis. Thereby, the number of conduction modes reduces to the number of bands crossing at the Fermi level. Hence, $\xi \approx 2N_{ch}l_e$,³⁷ with $N_{ch} = 2$, for the (10,10) nanotube. The localization length is consequently estimated to be $\xi \sim 5 \mu\text{m}$ so that it is typically larger than or similar to the nanotube length and thus strong localization effects (such as an insulating regime) are unlikely to be expected in pure SWNT's. Note that recent experimental work by Sumanakera *et al.*³⁸ has reported significant sensitivity to oxygen, which was shown to modify the conductivity by about 10%.

With respect to the magnetic field, renormalization group arguments suggest that the localization lengths will be weakly affected by the magnetic field³⁹ in quasi-1D systems. However, transport properties may be affected by the dephasing magnetic length $l_m = \sqrt{\hbar/eB}$, which is $l_m = 25.66$ nm or 8 nm, respectively, for $B = 1$ T or $B = 10$ T. Two cases may be distinguished whenever the mean free path is much larger than the nanotube circumference. Indeed, following Beenakker and Van Houten⁴⁰ and noticing that in the case of a nanotube, the cross section of the quantum wire reduces to $\lambda_F/2$, the magnetic phase relaxation time τ_B for weak and strong magnetic field limits can be written as follows (for $\lambda_F \ll l_e$):

$$\tau_B \approx \begin{cases} 12 \left(\frac{l_m}{\lambda_F} \right)^2 \tau_e & \text{if } l_m \ll \sqrt{\frac{\lambda_F l_e}{2}} \\ 128 \left(\frac{l_m^4}{\lambda_F^3 l_e} \right) \tau_e & \text{if } l_m \gg \sqrt{\frac{\lambda_F l_e}{2}} \end{cases} \quad (16)$$

So for the considered (9,0) and (10,10) tubes, we find that $\sqrt{\lambda_F l_e/2} \sim 18.24$ nm and 25.8 nm, respectively [we take $\lambda_F = 0.74$ nm (Ref. 12) and $W = 0.2078$ eV (Ref. 35)]. Hence, for $B = 1$ T, we conclude that $l_m \simeq \sqrt{\lambda_F l_e/2}$, which is an intermediate situation between low and strong magnetic fields, and no analytical expression of τ_B can be deduced, whereas $B = 10$ T is closer to the strong magnetic field limit where magnetic phase relaxation can be estimated analytically by

$$\tau_B = \frac{12\gamma_0\hbar}{(\lambda_F W)^2} l_m^2 \sqrt{n^2 + m^2 + nm}, \quad (17)$$

which gives for the (10,10) armchair nanotube a dephasing rate of $\tau_B \sim 2.8 \times 10^{-11}$ s. This means that for a (10,10) armchair tube, the electronic phase is randomized by a 10 T magnetic field roughly every 30 ps, which indicates that in the strong-field limit, the dephasing rate due to a magnetic field is just a few times the mean free times (we find $\tau_B/\tau_e \sim 3.14$ with the aforementioned parameters), so that τ_B should significantly contribute to damping the quantum interferences in the weak localization regime. Actually, both the mean free time and the magnetic dephasing rate scale linearly with diameter.

An analytical estimate of the electron-phonon inelastic scattering rate by Jishi *et al.*⁴¹ (τ_{el-ph}) gives at room temperature $\tau_{el-ph} \simeq (1-2) \times 10^{-12}$ s, which has to be compared with recent 20 ps, obtained by femtosecond time resolved experiments.⁴² Both values are slightly lower than our estimate magnetic dephasing coherence time, which would suggest a stronger contribution of the electron-phonon dephasing mechanism. We also note that inelastic dephasing

rates due to electron-phonon coupling have been recently evaluated by Suzuura and Ando,⁴³ and an interesting chirality-dependent dominant inelastic backscattering mechanism (breathing, stretching versus twisting²) was revealed.

Finally, with regard to the experimental results,¹⁷ one notices that if electronic transport is conveyed only by the outer shell of a metalliclike nanotube, as the magnetic field tends to decrease the TDOS at discrete values of the magnetic field corresponding to $(2n+1)/2\phi_0$ with integer n , an increase of resistance may follow from increasing the magnetic field. However, the short electronic coherence lengths that are observed in a magnetic field, the negative magnetoresistance and the $\phi_0/2$ Aharonov-Bohm oscillatory pattern are unlikely to be fully due to spectral effects (on the density of states), and a calculation of diffusion coefficients is mandatory to account for interferences between propagating electronic pathways in the nanotube structure. A recent study of the conductivity based on the Kubo formula has been performed in Ref. 44 and gives a geometrical explanation for the enhanced backscattering in MWNT's.

ACKNOWLEDGMENTS

S.R. acknowledges the European NAMITECH Network for financial support [ERBFMRX-CT96-0067 (DG12-MITH)]. Part of the work by R.S. is supported by a Grant in Aid for Scientific Research (No. 11165216) from the Ministry of Education and Science of Japan and the Japan Society for the Promotion of Science for the international collaboration. The MIT authors acknowledge support under NSF Grants Nos. DMR 98-04734 and INT 98-15744.

*Corresponding author. Email: roche@drfmc.ceng.cea.fr

[†]On leave from the Department of Physics and Department of Electrical Engineering and Computer Science, Massachusetts Institute of Technology, Cambridge, Massachusetts 02139.

¹S. Iijima, *Nature (London)* **354**, 56 (1991).

²R. Saito, G. Dresselhaus, and M.S. Dresselhaus, *Physical Properties of Carbon Nanotubes* (Imperial College Press, London, 1998).

³Y. Zhang *et al.*, *Science* **285**, 1719 (1999).

⁴H.T. Soh *et al.*, *Appl. Phys. Lett.* **75**, 627 (1999).

⁵J.C. Charlier, T.W. Ebbesen, and Ph. Lambin, *Phys. Rev. B* **53**, 11 108 (1996).

⁶S.G. Louie, S. Froyer, and M.L. Cohen, *Phys. Rev. B* **26**, 1738 (1982).

⁷Y. Saito, S. Uemura, and K. Hamaguchi, *J. Appl. Phys.* **37**, L346 (1998).

⁸J.W.G. Wildöer, L.C. Venema, A.G. Rinzler, R.E. Smalley, and C. Dekker, *Nature (London)* **391**, 59 (1998).

⁹R. Martel, T. Schmidt, H. Shea, T. Hertel, and Ph. Avouris, *Appl. Phys. Lett.* **73**, 2447 (1998).

¹⁰S.J. Tans, R.M. Verschueren, and C. Dekker, *Nature (London)* **393**, 49 (1998).

¹¹L. Venema *et al.*, *Nature (London)* **396**, 52 (1999).

¹²A. Rubio *et al.*, *Phys. Rev. Lett.* **82**, 3520 (1999).

¹³R. Saito, G. Dresselhaus, and M.S. Dresselhaus, *Phys. Rev. B* **61**, 2981 (2000).

¹⁴L. Langer *et al.*, *Phys. Rev. Lett.* **76**, 479 (1996).

¹⁵C. Naud, G. Faini, D. Mailly, and H. Pascard, *C. R. Acad. Sci., Ser. Iib: Mec., Phys., Chim., Astron.* **327**, 945 (1999).

¹⁶H.R. Shea, R. Martel, and Ph. Avouris, *Phys. Rev. Lett.* **84**, 4441 (2000).

¹⁷A. Bachtold *et al.*, *Nature (London)* **397**, 673 (1999).

¹⁸A. Fujiwara *et al.*, *Phys. Rev. B* **60**, 13 492 (1999).

¹⁹H. Ajiki and T. Ando, *J. Phys. Soc. Jpn.* **65**, 505 (1996).

²⁰C.H. Olk and J.P. Heremans, *J. Mater. Res.* **9**, 259 (1994).

²¹P. Kim, T. Odom, and J.L. Huang, *Phys. Rev. Lett.* **82**, 1225 (1999); **82**, 1225 (1999).

²²T.W. Odom *et al.*, *Nature (London)* **391**, 62 (1998).

²³H. Ajiki and T. Ando, *J. Phys. Soc. Jpn.* **62**, 1255 (1993); T. Ando, *Semicond. Sci. Technol.* **15**, R13 (2000).

²⁴W. Tian and S. Datta, *Phys. Rev. B* **49**, 5097 (1994).

²⁵J.P. Lu, *Phys. Rev. Lett.* **74**, 1123 (1995).

²⁶S. Roche and R. Saito, *Phys. Rev. B* **59**, 5242 (1999).

²⁷M. Ichida, *J. Phys. Soc. Jpn.* **68**, 3131 (1999).

²⁸J.M. Mintmire and C.T. White, *Phys. Rev. Lett.* **81**, 2506 (1998).

²⁹H. Kataura *et al.*, *Synth. Met.* **103**, 2555 (1999).

³⁰L. Chico, L.X. Benedict, S.G. Louie, and M.L. Cohen, *Phys. Rev. B* **54**, 2600 (1996).

³¹M.P. Anantram and T.R. Govindan, *Phys. Rev. B* **58**, 4882 (1998).

³²T. Kostyrko, M. Bartkowiak, and G.D. Mahan, *Phys. Rev. B* **60**, 10 735 (1999).

³³K. Harigaya, *Phys. Rev. B* **60**, 1452 (1999).

³⁴S. Frank, P. Poncharal, Z.L. Wang, and W.A. de Heer, *Science* **280**, 1744 (1998).

- ³⁵C.T. White and T.N. Todorov, *Nature (London)* **393**, 240 (1998).
- ³⁶D.J. Thouless, *Phys. Rev. Lett.* **39**, 1167 (1977).
- ³⁷K.B. Efetov and A.I. Larkin, *Zh. Éksp. Teor. Phys. [Sov. Phys. JETP]* **58**, 444 (1983).
- ³⁸G.U. Sumanakera *et al.*, *Phys. Rev. Lett.* **85**, 1096 (2000).
- ³⁹I.V. Lerner and Y. Imry, *Europhys. Lett.* **29**, 49 (1995).
- ⁴⁰C.W.J. Beenakker and H. van Houten, *Phys. Rev. B* **38**, 3232 (1988).
- ⁴¹R.A. Jishi, M.S. Dresselhaus, and G. Dresselhaus, *Phys. Rev. B* **48**, 11 385 (1993).
- ⁴²T. Hertel and G. Moos, *Phys. Rev. Lett.* **84**, 5002 (2000).
- ⁴³H. Suzuura and T. Ando, *Mol. Cryst. Liq. Cryst.* **340**, 731 (2000).
- ⁴⁴S. Roche *et al.* (unpublished).